Computers & Geosciences 90 (2016) 131–143

Contents lists available at ScienceDirect

Computers & Geosciences

journal homepage: www.elsevier.com/locate/cageo

LORICA – A new model for linking landscape and soil profile evolution: Development and sensitivity analysis

Arnaud J.A.M. Temme [a,b,*], Tom Vanwalleghem [c]

[a] Environmental Sciences, Wageningen University, The Netherlands
[b] Institute for Arctic and Alpine Research, University of Colorado, United States
[c] Department of Agronomy, University of Cordoba, Spain

ARTICLE INFO

Article history:
Received 3 February 2015
Received in revised form
13 August 2015
Accepted 15 August 2015
Available online 18 August 2015

Keywords:
Soilscape
Soil–landscape modelling
Soil modelling
Landscape evolution modelling
Sensitivity analysis
LORICA

ABSTRACT

Soils and landscapes evolve in tandem. Landscape position is a strong determinant of vertical soil development, which has often been formalized in the catena concept. At the same time, soil properties are strong determinants of geomorphic processes such as overland erosion, landsliding and creep. We present a new soilscape evolution model; LORICA, to study these numerous interactions between soil and landscape development. The model is based on the existing landscape evolution model LAPSUS and the soil formation model MILESD. The model includes similar soil formation processes as MILESD, but the main novelties include the consideration of more layers and the dynamic adaption of the number of layers as a function of the soil profile's heterogeneity. New processes in the landscape evolution component include a negative feedback of vegetation and armouring and particle size selectivity of the erosion–deposition process. In order to quantify these different interactions, we present a full sensitivity analysis of the input parameters. First results show that the model successfully simulates various soil–landscape interactions, leading to outputs where the surface changes in the landscape clearly depend on soil development, and soil changes depend on landscape location. Sensitivity analysis of the model confirms that soil and landscape interact: variables controlling amount and position of fine clay have the largest effect on erosion, and erosion variables control among others the amount of chemical weathering. These results show the importance of particle size distribution, and especially processes controlling the presence of finer clay particles that are easily eroded, both for the resulting landscape form as for the resulting soil profiles. Further research will have to show whether this is specific to the boundary conditions of this study or a general phenomenon.

1. Introduction

Soils and landscapes are closely interrelated. Their genesis, their present state, but also their future evolution are a result of dynamic interactions. Vertical soil profile development and soil spatial distribution are both controlled by fluxes of water, chemicals, energy and sediment. All these fluxes are controlled by the form of the landscape surface but also by subsurface heterogeneities, such as impermeable layers. In most landscapes, soil erosion and sediment redistribution are the main processes that continuously change this landscape surface and the depth and properties of underlying soils. However, the soil properties themselves control landscape development significantly as well. Erosion rates can change over several orders of magnitude depending on soil erosivity or rock type, or small textural changes can induce differences in infiltration rates that in turn control water fluxes. Recent research has clearly shown the effect of opposing aspects on weathering rates and critical zone architecture (Anderson et al., 2014).

Because of the importance of these interactions, recent studies have focused on linking soil and landscape processes and their feedbacks through modelling, in so-called landscape–soilscape models. Minasny et al. (in press) made a recent review of presently available soil–landscape models. Early models were limited to simulating the formation and redistribution of a thin layer of regolith (e.g. Minasny and McBratney, 1999), that was generated through a simple soil production or bedrock weathering function. More recently, more advanced models were introduced that are also able to track soil and sediment properties over time. For example, mARM3D by Cohen et al. (2010) is a model that simulates soil evolution in a three-dimensional landscape and includes some important soil formation processes, especially focusing on particle size-grading and effects of surface armouring due to erosion. Physical weathering rates have been shown to vary strongly with

* Corresponding author at: Environmental Sciences, Wageningen University, The Netherlands.

http://dx.doi.org/10.1016/j.cageo.2015.08.004
0098-3004/

landscape position. For example, a model by Anderson et al. (2013) of landscape evolution driven by frost processes produced striking aspect differences in weathering depth and sediment generation. Finke et al. (2013) used the pedon-scale model Soilgen2 at 108 sites in a 1329 ha forest site in order to extract statistical soil–landscape relations. By running different model scenarios, they were able to demonstrate the importance of bioturbation for controlling soil formation and soil morphology at the landscape scale. Finally, the model MILESD by Vanwalleghem et al. (2013) proposes a full integration of all main soil forming processes with a landscape evolution model. This model includes processes ranging from physical and chemical weathering, clay translocation to bioturbation. MILESD was used successfully to simulate the evolution of important soil properties such as texture, bulk density or stoniness on soil catenas in Australia over time and under different erosion scenarios. Additionally, this model also keeps track of the exported sediment properties, opening important links to the geomorphology community to assess the effects of changing climate or soil conditions on the sediment record. This model was one of the first to highlight the potential of linking soil and landscape processes for explaining complex feedbacks, although in its present form it holds some limitations. The landscape evolution model used in MILESD is a simplified cellular automata approach, including diffusive and concentrated water erosion processes, sediment deposition and selectivity. In order to fully exploit the potential of soil–landscape coupling, MILESD would benefit from coupling with a more complex landscape evolution model, one that also includes other processes such as mass wasting or an explicit representation of flow routing and sediment transport capacity. In addition, for computational reasons, MILESD is made up out of 4 layers (bedrock plus three soil layers), which is logical from a soil's perspective with a typical A–B–C profile, but has some drawbacks for universal application and for validation against numerical field data.

Therefore, in this study we propose a new, upgraded model called LORICA, that links the soil formation module of MILESD with aspects of landscape evolution model LAPSUS (Schoorl et al., 2014; Schoorl and Veldkamp, 2001). The objective of this paper is first to present this new model, second to evaluate model behaviour on a hypothetical landscape and third to exhaustively test model sensitivity to input parameter variation by means of a global sensitivity analysis.

2. Model

The geomorphic evolution in LORICA is similar to the geomorphic evolution in LAPSUS and many other landscape evolution models in the sense that multiple geomorphic processes interact through the changes they make to the landscape (Temme et al., 2011; Temme and Veldkamp, 2009). However, it differs in some of the core erosion process descriptions as will be detailed below, to take full advantage of the fact that grain size information can be incorporated in the erosion and deposition process. Vertical profile evolution in LORICA is similar to profile evolution in MILESD (Vanwalleghem et al., 2013), particularly where the choice of pedomorphic processes and process descriptions is concerned. Here, the main difference lies in the number of subsurface layers that is simulated. In MILESD, the number of layers is fixed at four; three soil layers and a bedrock layer (Vanwalleghem et al., 2013). In LORICA, it is an order of magnitude larger and excludes the bedrock. Also new in LORICA is the introduction of dynamic layering as soil heterogeneity appears or disappears as a function of soil and landscape dynamics. Therefore, in LORICA, soil horizons are emergent properties that typically span multiple simulated layers whereas in MILESD the simulated layers are soil horizons. The model has annual temporal resolution, to allow simulations over the millennial temporal extents over which soilscapes evolve (Förster and Wunderlich, 2009; Sommer et al., 2008).

2.1. Soilscape architecture

The soilscape in LORICA is discretized into a regular grid of square cells that each have an altitude value. This altitude value represents the surface topography. In each cell, a user-specified number of soil-layers is defined with variable and dynamic thickness. In this study, 22 layers were selected. Layers are assumed to be internally homogenous, and bedrock, which starts under the lowest soil layer, is also assumed homogenous.

In each layer, the mass of material in each of five grain size classes and two organic matter classes is recorded. Like in MILESD, the texture classes are coarse material (2.10^{-3}–10.10^{-3} m), sand (50.10^{-6}–2.10^{-3} m), silt (2.10^{-3}–50.10^{-6} m), clay (1.10^{-7}–2.10^{-6} m) and fine clay ($< 1.10^{-7}$ m). Class limits are derived from the USDA classification (Soil Survey Staff, 1999) with the exception of the coarse class and the fine clay class. The coarse class was added to reflect the transition from bedrock to soil in the form of saprolite – broken rock (Vanwalleghem et al., 2013). The underlying assumption is that soil forming processes start only after bedrock is broken up into loose coarse particles. The fine clay class was added because of its importance in clay translocation processes (Barshad, 1959). Organic matter is divided into quickly decomposing organic matter and slowly decomposing organic matter, to reflect the basic dynamics of soil organic matter in developing soils (Braakhekke et al., 2011).

Layer bulk density is calculated with pedotransfer functions based on the mass fractions of the various grain size classes and the organic matter in each layer. This implies that strain effects, or the volume expansion of bedrock during the weathering process, are taken into account implicitly through the effect on multiple soil forming processes on the grain size distribution. A large number of pedotransfer functions to calculate bulkdensity is available for various settings (McBratney et al., 2002; Pachepsky et al., 2006), although a globally valid function remains elusive. For this study, where organic matter contents remained low, a pedotransfer function from Tranter et al. (2007) was selected

$$\rho_f = 1000\,(1.35 + 0.00452\,(\text{sand\_frac} + 0.76\text{silt\_frac}) + (\text{sand\_frac} + 0.76\text{silt\_frac} - 44.65)^2 - 0.0000614 \quad (1)$$

where ρ_f is bulk density of the fine earth fraction [kg m^{-3}], sand_frac and silt_frac are the mass fractions of sand and silt in the fine earth fraction [kg kg^{-1}]. Note that in this pedotransfer function, compaction effects are assumed neglible and that therefore depth below the soil surface or overlying soil mass are not factors in Eq. (1). Correction for the coarse fraction was performed with Vincent and Chadwick's (1994) formula

$$\rho_s = \frac{\text{total soil}}{\left(\frac{\text{fine earth}}{\rho_f} + \frac{\text{coarse}}{\rho_r}\right)} \quad (2)$$

where ρ_s is overall soil bulk density [kg m^{-3}] and ρ_r is the bulk density of the coarse fraction, which was set at 2700 kg m^{-3} for the present study. Total soil is the total soil mass [kg], equal to the sum of fine earth and coarse mass (fine earth, coarse).

Layer thickness is calculated from the bulk density and the total mass of material in a layer and is allowed to vary between timesteps due to geomorphic or pedological development, until a user-specified minimum or maximum thickness is reached. For the top layer, no minimum thickness is defined and for the bottom layer, no maximum thickness is defined. If a layer becomes thinner than the user-specified minimum, it is combined with either the

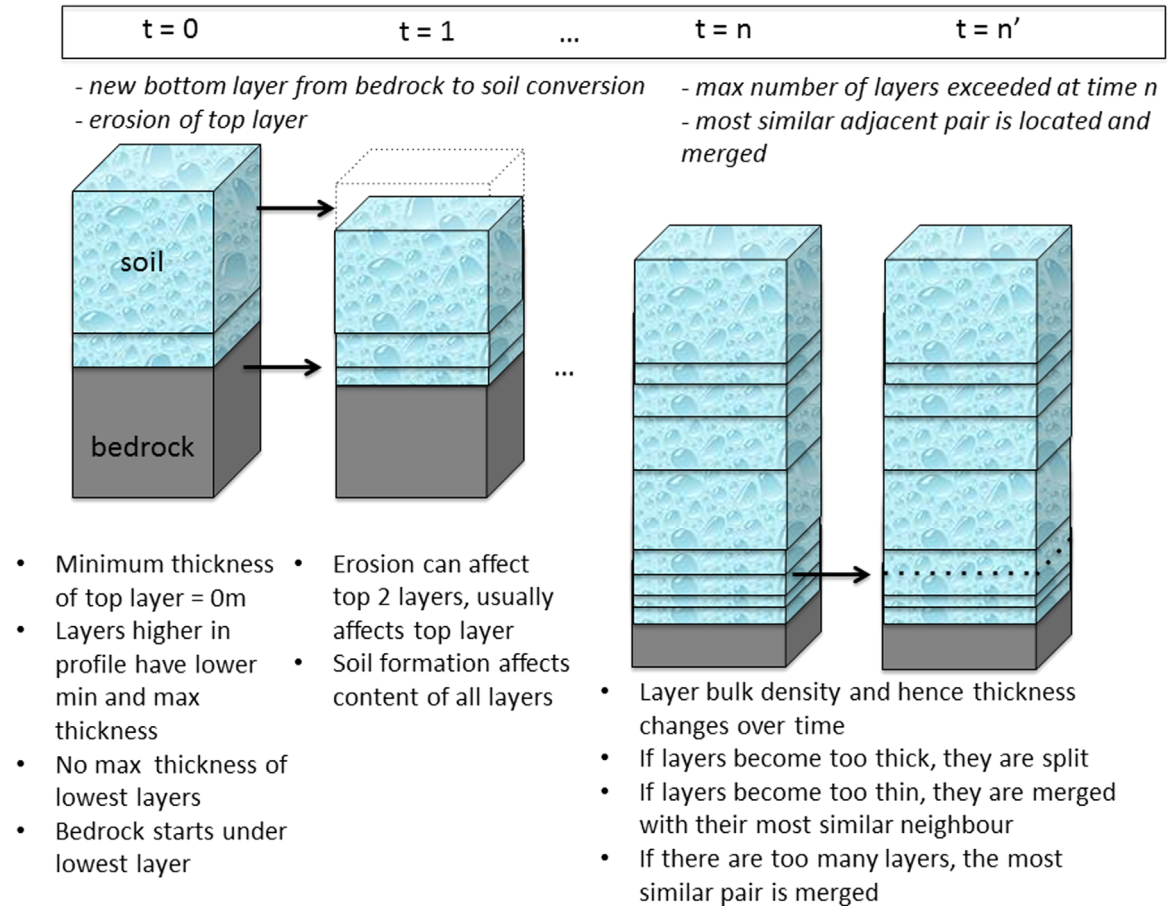

Fig. 1. Illustration of variable and dynamic layering rules of the subsurface in LORICA.

overlying or the underlying layer – whichever is most similar to it in terms of its soil properties. If a layer grows thicker than the user-specified maximum, it is split into two equally thick layers with the same properties. If the total number of layers grows larger than a user-specified maximum, then a search algorithm merges the two layers that are most similar to each other, without violating maximum thickness rules (Fig. 1).

The architecture with variable and dynamic thickness of layers is perceived to be widely applicable and somewhat more practical than alternatives where the number of soil layers equals the number of timesteps in the model (Salvador-Blanes et al., 2007), or where the number of layers is fixed (Vanwalleghem et al., 2013). This is because LORICA's layers essentially keep track of the same material on its way from bedrock to the surface in eroding situations, or on its way from surface to deeper layers in depositing situations and hence minimizes the loss of information associated with having layers that are internally homogenous. The layering architecture adapts to have thinner layers in zones where vertical variation is largest, and allows for instance a detailed recording of variation in palaeosols buried under a thick layer of undifferentiated sediment. Conversely, in areas with homogeneous material, the number of layers is low, which benefits computational efficiency.

For this study, 22 initial subsurface layers were defined, which were initially 5 cm thick between 0 and 50 cm from the surface, 25 cm think between 50 and 250 cm from the surface and 100 cm thick from 250 cm down to 550 cm from the surface. The lowest layer covered the rest of the soil parent material to the bedrock interface. The maximum number of layers was set at 30.

2.2. Hydrology

LORICA only deals with water in the landscape explicitly where overland water flow is concerned. A standard kinematic wave approach is used. In this simplification of the St-Venant equations, waterflow is driven only by gravitational forces, not by pressure gradients, inertia or acceleration or deceleration. This simplification appears acceptable at watershed scale where acceleration or deceleration are small and where local slopes are larger than the change in water depth downstream (Tucker and Hancock, 2010). Note that for this reason, in the kinematic wave approach it is impossible to simulate some aspects of fluvial depositionary environments such as true floodplains or levee breaches. Fluvially-oriented models such as CAESAR (Coulthard and Van de Wiel, 2006; Van de Wiel et al., 2007) are more suited for such environments. Depressions, even in an eroding landscape, need to be dealt with outside of the kinematic wave approach. LORICA is equipped to do this due to its similarity with LAPSUS where a depression algorithm has been implemented (Temme et al., 2006).

The amount of water available for overland flow at each yearly time step is calculated as

$$Q = Q_{in} + (\text{Rainfall} - \text{Evap} - \text{Infil}).\ \text{cellsize}^2 \quad (3)$$

Where Q is overland flow [m^3], Q_{in} is overland flow contributed from upslope cells [m^3], Rainfall is annual rainfall [m], Evap is annual evaporation [m], and Infil is annual infiltration [m]. The routing of overland flow Q over cells in the soilscape is calculated with multiple flow (Freeman, 1991; Holmgren, 1994):

$$f_i = \frac{\Delta_i{}^p}{\sum_{j=1}^{\max 8} (\Delta_j{}^p)} \quad (4)$$

where f_i is the fraction of flow from a cell into its downslope neighbour i, Δ is slope gradient and p is an exponent which determines to which extent flow is divergent. For $p=\infty$, all water is routed to the steepest downslope neighbour. For $p=0$, water is divided equally over all (maximum 8) downslope neighbours. Multiple flow algorithms have the advantage that they can simulate divergent flow on convex landforms, but have computational disadvantages – particularly the fact that so far they do not benefit from the inherent stability of implicit mathematical solutions (Goren et al., 2014). The main impact of this lacking inherent stability is that multiple flow models such as LORICA must run at smaller temporal resolution, or larger spatial resolution. To solve Eq. (4), all cells in the DEM are sorted before every timestep and calculations start at the top cell.

Subsurface flow in LORICA is not modelled explicitly. This means that the pedomorphic processes cannot benefit from simulations of the liquid phase (such as in SoilGen2, Finke and Hutson (2008)). In other words, LORICA assumes that soils are freely drained, and that the ground water table and reduction play no role in weathering, bioturbation and clay translocation processes.

2.3. Vegetation

In the currently presented version of LORICA, vegetation only affects the erosion process through its protection of the surface. Simulation of effects on organic matter dynamics and on bioturbation has also been implemented but was not included in the current study to reduce the number of variables to be included in sensitivity analysis.

2.4. Geomorphic processes

LORICA simulates erosion and deposition due to water erosion, creep, tillage and landsliding. In addition, it simulates bedrock weathering into the coarse grain size class and simplified tectonics (tilting and uplift). In the present study, only advection, i.e. erosion and deposition as a result of overland flow, is presented and simulated (Fig. 2).

Advection is usually simulated either as a detachment-limited process, where material that is detached from the surface, is eroded by definition (hence, no redeposition), or as a transport-limited process, where erosion and deposition are only a function of transport capacity for sediment (hence, instantaneous erosion or deposition upon changes in transport capacity). In the detachment-limited approach, there is no limit to the amount of sediment in transport (i.e. there is no transport limitation). In the transport-limited approach, there is no limit to the speed of uptake of sediment once erosion is required, or on the speed of deposition once deposition is required (i.e. there is no detachment or re-attachment limitation). In the context of generic soilscape evolution, both these end-member models are unrealistic. Spatial differences in topsoils will affect erodibility and hence detachment rates, differences in the grain size of material in transport will affect redeposition rates, and footslopes and valleys must be able to experience deposition.

Therefore, in LORICA we have taken an approach where the sediment transport capacity is compared to the total amount of sediment in transport at every transition between cells. To do this, a mass balance is calculated for sediment in the streamflow. Erosion can happen if more sediment can be transported than is in transport, and deposition can happen if more sediment is in transport than can be transported. In this respect, this method is equivalent to the water erosion and deposition algorithm in LAPSUS (Schoorl et al., 2002), and is a ξ–q model *sensu* Davy and Lague (2009): a model that is both detachment and transport limited.

Different from LAPSUS, in LORICA, the transport limitation is provided by the commonly used stream power equation:

$$TC = K\, q^m\, \Delta^n \quad (5)$$

where TC is the transport capacity for sediment [kg y^{-1}], K is a

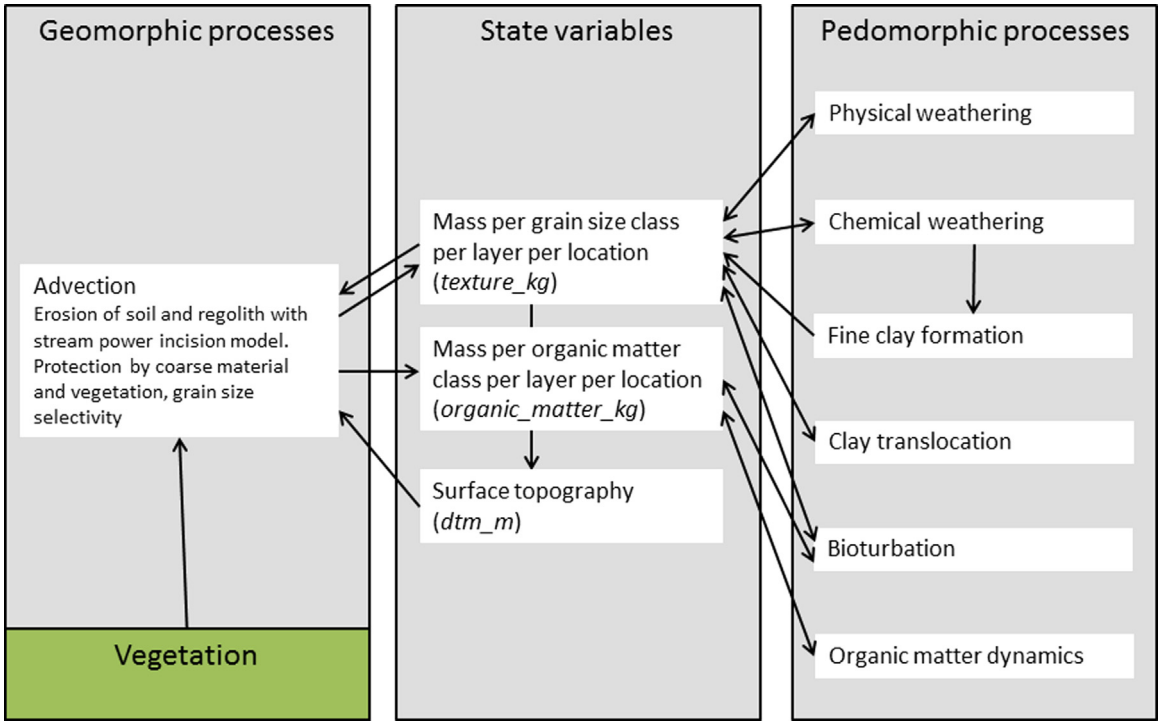

Fig. 2. Processes and state variables of LORICA in the present study.

constant relating stream power to amount of sediment (Tucker and Hancock, 2010), q is the amount of flow per unit cell width [$m^3\ m^{-1}$], and Δ is slope gradient [–]. Constants m and n are empirically determined, and typically have values between 1 and 2. Transport capacity TC is compared to the amount of sediment in transport S [$kg\ y^{-1}$]:

$$S = \sum_{i=0}^{6} S_i \tag{6}$$

where S_i is the sediment in transport in each of the five texture classes and the two organic matter classes. Erosion can occur when transport capacity exceeds the amount of sediment in transport by more than a user-defined threshold TC_{min} [kg] (cf. Shields, 1936). If that is the case, it is further limited by surface armouring by the largest size class (Parker and Klingeman, 1982) and vegetation protection:

$$E_{pot} = (TC - S)\ e^{-c1\ \mathrm{coarse\_frac}}\ e^{-c2\ \mathrm{plant\_frac}} \tag{7}$$

where E_{pot} [$kg\ y^{-1}$] is potential erosion, coarse_frac [–] is the mass fraction of the coarse grain size class in the top layer, plant_frac [–] is the fraction of the surface covered by vegetation (Collins et al., 2004), and $C1$ and $C2$ are parameters expressing the extent of protection against erosion by respectively rocks or vegetation. No erosion occurs in locations where the top soil layer is completely composed of the coarse size fraction, or completely protected by plants.

In order to handle grain size selectivity effects during erosion–deposition, LORICA uses a simplified approach, similar to MILESD, as water flow is not resolved at a sufficiently small temporal resolution to do this in more detail. Further detailing the ξ–q model (Davy and Lague, 2009), selective transport is used to determine how E_{pot} is composed of the five grain size classes:

$$E_{pot,\,i} = \frac{\mathrm{size}_i^{-b1}}{\sum_{j=0}^{4} \mathrm{size}_j^{-b1}}\, E_{pot} \tag{8}$$

where $size_i$ is the size of grain size class i and $b1$ is a variable with value >0. A larger fraction of potential erosion is taken from grain size class i when its size is smaller, and when $b1$ is small. The value of $b1$ is calculated as:

$$b1 = 0.5\ e^{\mathrm{selcst\ TC}} \tag{9}$$

For selectivity constant (selcst)=1, $b1$ approaches a value of 0.5 for very small transport capacities, but increases with increasing transport capacities. This reflects the fact that larger transport capacities (i.e. stronger flows) are less selective. Larger values of *selcst* cause increased size selectivity, smaller values cause decreased size selectivity. This formulation is functionally equivalent to the Hjulström curve (Hjulström, 1935) which relates the minimum flow velocity before deposition or erosion occurs to grain size. A difference with the Hjulström curve is that in LORICA it is not harder to erode cohesive sediments such as clays. This choice was made because for the moment we assume that in LORICA sediments will be always mixed and hence that the cohesive potential of clay particles is not realized. For size selectivity, both organic matter fractions are assumed to behave as fine clay.

Ultimately, $E_{pot,\,i}$ [$kg\ y^{-1}$] is eroded from the mass of grain size class i present in the top soil layer and added to S_i. The erosion formulation can result in $S < TC$, or undersaturated flow, if the mass in any grain size class i is less than $E_{pot,\,i}$, or if surface protection by the coarse fraction or by vegetation is substantial. Both of these causes constitute detachment limitation.

Deposition can occur when overall transport capacity TC is less than sediment in transport S. In this case, transport capacity TC_i [$kg\ y^{-1}$] for each grain size class is also calculated using a selectivity fraction

$$TC_i = TC\ \frac{\mathrm{size}_i^{-0.5}}{\sum_{j=0}^{4} \mathrm{size}_j^{-0.5}} \tag{10}$$

where $size_i$ is the mean particle size for grain size class i. This results in smaller transport capacities for larger grain sizes, which reflects the fact that sediment travel distances are smaller for heavier particles. Also this formulation is functionally equivalent to the Hjulström curve (Hjulström, 1935). Larger grain sizes are deposited already at larger flow velocities. Organic matter is assumed to have the same TC_i value as fine clay. Deposition in the top soil layer results if there is more sediment or organic matter in transport (S_i) than can be transported (TC_i)

$$\Delta M_{i,0} = S_i - TC_i \tag{11}$$

where $\Delta M_{i,0}$ is the change in the mass of grain size class i in the top layer (layer 0) [kg]. Deposition in the five grain size classes will cause the top soil layer to change its mass, its bulk density and in some cases to exceed the maximum thickness. In the latter case, the layer will be split as described above. Note that after deposition has occurred, the overall sediment in transport S can still remain larger than TC. Such oversaturated flow is more likely to occur when finer size classes dominate the sediment in transport. Numerically, incomplete deposition helps avoid, rather than promote model instability that could results from instantaneous deposition of the complete amount of sediment S–C (Schoorl et al., 2014).

2.5. Soil forming processes

LORICA's processes of soil formation for the present study include physical weathering, chemical weathering, fine clay formation and translocation, bioturbation and organic matter dynamics.

Physical weathering is seen as the second step in the weathering process: the first, weathering of bedrock into the coarse size class is seen as a geomorphic process and was not simulated in the present study. Physical weathering in LORICA reduces the mass present in the coarse, sand and silt fractions in every layer, depending on the grain size class' mass, the layer's depth below the surface and the grain size

$$\Delta M_{pw\ i,l} = -\ M_{i,l}\ C3\ e^{C4\ \mathrm{depth_l}}\ \frac{C5}{\log \mathrm{size_i}} \tag{12}$$

where $\Delta M_{pw\ i,l}$ [kg] is the change in mass of grain size class i in layer l due to physical weathering. LORICA and its predecessor MILESD are asymmetrical models where the material fragmented by physical weathering is redistributed over two smaller size fractions of different size. Such models fit the rare available experimental data (of the salt-weathering fragmentation of chlorite schist, Wells et al., 2008). In our case, the proportion of each of the daughter size classes is calculated as proportional to the size of each class. Thus, one mass unit of coarse fragments breaks up into 0.975 units of sand and 0.025 units of silt. One mass unit of sand breaks up into 0.96 units of silt and 0.04 units of clay. Since field evidence suggests that fine clay is not formed through physical weathering (Chittleborough et al., 1984; Smeck et al., 1981), one mass unit of silt breaks up into a mass unit of (coarse) clay only.

Chemical weathering is a complex set of processes that features mineral-specific dissolution, oxidation or reduction. It depends of climatic and other site characteristics such as water availability (Maher, 2010). Reaction rates vary with depth due to gradients in temperature, pH and solutes in soil water, whereas transport rates with water to other soil layers depend on hydraulic conductivity and hence on soil texture, porosity and water content. LORICA is unable to resolve this inherent complexity, among others due to

Table 1
List of parameters for LORICA.

Symbol	Parameter	Unit	Equation	Proposed valid range	Reference value	Acronym for sensitivity analysis
Geomorphic parameters						
Water erosion and deposition						
p	Multiple flow factor	[dimensionless]	4	1–4	2	erop
m	Exponent of overland flow	[dimensionless]	5	1–2	1.5	erom
n	Exponent of slope	[dimensionless]	5	1–2	1.5	eron
K	Advection erodibility	[dimensionless]	5	0.0003–0.3	0.03	erok
TC_{min}	Erosion threshold	[kg]	–	0–0.3	0.03	erocrit
C1	Rock protection constant	[dimensionless]	7	0–2	1	eroc1
C2	Bio protection constant	[dimensionless]	7	0–2	1	eroc2
Selcst	Selectivity constant	[kg^{-1}]	9	0–2	1	erocsel
Soil formation parameters						
Physical weathering						
C3	Weathering rate constant	[y^{-1}]	12	$0–10^{-3}$	4.10^{-6}	pwc3
C4	Depth decay constant	[m^{-1}]	12	−0.25 to 1	−0.5	pwc4
C5	Particle size constant	[m]	12	4–6	5	pwc5
Chemical weathering						
C6	Weathering rate constant	[kg/m^2 mineral surface area/y]	13	$0–10^{-3}$	4.10^{-6}	cwc6
C7	Depth decay constant	[m^{-1}]	13	−0.25 to 1	−0.5	cwc7
C8	Specific area coefficient	[dimensionless]	13	0.5–2	1	cwc8
Clay translocation						
Cnf	Fine clay neoformation fraction	[dimensionless]	15	0–1	0.5	claycnf
C9	Depth constant 1	[m^{-1}]	15	0–4	1	clayc9
C10	Depth constant 2	[m^{-1}]	15	4–20	20	clayc10
Ctr	Maximum eluviation	[kg]	16,17		0.007	clayctr
C11	Saturation constant	[dimensionless]	16,17		2	clayc11
Bioturbation						
Bio_{pot}	Potential bioturbation	[kg/m^2/y]	18	0–20	6	biopot
C12	Depth decay rate	[m^{-1}]	18	0–5	2.5	bioc12
Carbon cycle						
ΔM_{SOMpot}	Potential organic matter input	[kg/m^2/y]	21	0–20	1.5	carbpot
C13	Depth limitation constant	[m^{-1}]	21	0–20	8	carbc13
f_{hum}	Humification fraction	[dimensionless]	–	0–1	0.8	carbfhum
C14	Decomposition rate quickly decomposable SOM	[y^{-1}]	22	0–0.1	0.01	carbf14
C15	Decomposition rate quickly decomposable SOM	[m^{-1}]	22	0–20	8	carbf15
C16	Decomposition rate slowly decomposable SOM	[y^{-1}]	23	0–0.1	0.005	carbf16
C17	Decomposition rate slowly decomposable SOM	[m^{-1}]	23	0–20	8	carbf17

the fact that it does not simulate the soil's liquid phase. Instead, it operates under the realization that water is likely most reactive and soils are most permeable at the top of the soil reactor (Anderson et al., 2007). Hence, as in MILESD, a simple formulation is used that relates chemical weathering rate linearly to specific surface area (*surf_area*) and exponentially to depth below the surface:

$$\Delta M_{cw\,i,l} = -C6\, M_{i,l}\, \text{surf\_area}_i\, C8\, e^{C7\,\text{depth}_l} \quad (13)$$

The exponential decline with depth reflects the fact that soil moisture variations that drive both dissolution and transport are larger close to the surface than deeper in the soil and fit an exponential function (Amenu et al., 2005). The determination of specific surface areas of minerals is not simple (Salvador-Blanes et al., 2007), and therefore the specific surface area in LORICA was lumped per grain size class and used as model input (Table 1). Hence, changes in the surface area of soil constituents as weathering progresses are not considered. The specific surface area of the coarse grain size class is so small that chemical weathering of the coarse fraction is not considered.

Next to the loss of mass from the various grain size classes that chemical weathering causes, LORICA considers two side-effects: the reduction in size of weathered particles and the neoformation of fine clay. To calculate the effect of smaller particles falling into smaller grain size classes, particles are approximated by spheres. The fraction f of the weathered mass from each grain size class i that falls into the next smaller grain size class $i+1$ is calculated as:

$$f = \frac{r_{i+1}^3}{r_i^3 - r_{i+1}^3} \quad (14)$$

where r, the radius of the spherical grain, is taken to be the grain size of grain size class i. Since grain sizes are model inputs, f is constant per grain size class. For sand, $f = 1.56 \times 10^{-5}$, for silt it is 6.40×10^{-5} and for clay it is 1.25×10^{-4}. More background on how these are calculated can be found in the MILESD model description (Vanwalleghem et al., 2013).

Clay neoformation is the formation of new clay minerals from the dissolved weathering products. In field settings, neoformation of clays is difficult to distinguish from translocation of clays, yet empirical evidence suggests that it is highest at some depth below the surface (Barshad, 1959). Therefore, clay neoformation is modelled in LORICA as in MILESD as a double exponential function of depth below the surface:

$$\Delta M_{nf\ \text{fine clay},l} = c_{nf}\left(e^{-c9\ \text{depth}} - e^{-c10\ \text{depth}}\right) \sum_{l=0}^{\max} \sum_{i=1}^{3} \left(\Delta M_{cw\,i,l}\right) \quad (15)$$

where Cnf [–] is the fine clay neoformation constant and the mass involved in chemical weathering from the sand, silt and (coarse) clay size classes is summed over all soil layers to obtain the mass

of dissolved weathering products available for neoformation. This formulation cannot at the moment resolve the change in neoformation of fine clay as mineral composition of the weathering soil constituents changes – which was observed in a chronosequence of soils in California (Maher et al., 2009).

Clay translocation in LORICA and MILESD is based on simulations by Legros (1982) in which a fixed quantity of clay is eluviated and illuviated at each time step. However, the fixed quantity ctr [kg] is reached only for a soil layer that purely contains fine clay:

$$\Delta M_{tr\ \text{fine clay}\,,\,l} = -\ c_{tr}\left(1 - e^{-\text{c11 fine clay\_frac}}\right) \tag{16}$$

$$\Delta M_{tr\ \text{fine clay},\,l+1} = c_{tr}\left(1 - e^{-\text{c11 fine clay\_frac}}\right) \tag{17}$$

Bioturbation in LORICA uses an approach similar to that of Yoo et al. (2011), where soil mixing is calculated between individual soil layers. In LORICA, as in MILESD, this is formulated as proportional to biological activity in the receiving layer, and inversely proportional to the distance between layers.

First, the total mass of soil material in a cell that is bioturbated, Bio [kg], is calculated

$$\text{Bio} = \text{Bio}_{\text{pot}}\left(1 - e^{-\text{c12 soil thickness}}\right)\text{cellsize}^2 \tag{18}$$

where Bio_{pot} is the potential bioturbation rate [kg m^{-2}] for soils without depth limitation, cellsize is the grid cell size [m] and $c12$ [m^{-1}] is a parameter determining how quickly bioturbation decreases with soil thickness. This exponential decline with depth is supported by experimental data of earth-worm activity (Canti, 2003). Then, the total bioturbated mass is calculated per layer. Integrating over (18) between the top and bottom of a layer gives an index for bioturbation [–]

$$\text{Index}_{\text{bio,l}} = \frac{1}{c12}\left(e^{-c12\ \text{bottom}_l} - e^{-c12\ \text{top}_l}\right) \tag{19}$$

This index is then divided by the similarly calculated index for the entire soil thickness, Bio_{soil}, and multiplied with the total mass of bioturbated material *Bio*, to calculate the mass of bioturbated material received in and moved from layer *l*, $\Delta M_{bio,\,l}$ [kg]

$$\Delta M_{bio,\,l} = Bio\ \frac{\text{Index}_{\text{bio, l}}}{\text{Index}_{\text{bio, soil}}} \tag{20}$$

Exchange of fractions of $\Delta M_{bio,l}$ with other soil layers is proportional to the distance to the other layer in the soil profile and to the mass of the other layer. This has the effect that less bioturbated material is exchanged with thinner layers, and with layers that are further removed. It is assumed that bioturbation results only in the exchange of sand, silt, clay and organic matter between layers, which means that the coarse fraction is unaffected. This can result in stone lines at depth in the soil.

Organic matter dynamics are simulated similar as in earlier models (Minasny et al., 2008; Vanwalleghem et al., 2013; Yoo et al., 2006), where the balance of organic matter in the quickly decomposing and slowly decomposing fractions is equal to production and mixing inputs, minus losses due to decomposition and erosion. Mixing and erosion are simulated in the bioturbation and advection modules of the model respectively. Production in LORICA is determined by a base rate of production, and varies with depth below the surface (Baisden et al., 2002; Ewing et al., 2006; Yoo et al., 2006). The rate of production ΔM_{SOM} [kg] is calculated as:

$$\Delta M_{SOM}\,\Delta M_{SOMpot}\left(1 - e^{-\text{c13 soil thickness}}\right)\text{cellsize}^2 \tag{21}$$

Where ΔM_{SOMpot} [kg m^{-2}] is the potential input of soil organic matter, and $c12$ is a variable determining the decrease of input with soil thickness [m^{-1}]. Similarly to the calculation of bioturbation, the distribution of ΔM_{SOMpot} over the layers in the soil profile is calculated by integration of (21) between top and bottom of a layer, relative to integration over the entire profile thickness. Finally, as in MILESD, the division of input in a layer between quickly and slowly decomposing soil organic matter per layer is calculated with a humification fraction (f_{hum}).

Decomposition is calculated as a function of depth below the soil surface, and is different for the quickly and slowly decomposing organic matter pools:

$$\Delta M_{SOMyoung,\,l} = -\,c14\ M_{SOMyoung,\,l}\ e^{-\text{c15 depth}_l} \tag{22}$$

$$\Delta M_{SOMold,\,l} = -\,c16\ M_{SOMold,\,l}\ e^{-\text{c17 depth}_l} \tag{23}$$

The full list of model parameters is provided in Table 1. In this table, the last column indicates the acronym that was used in the sensitivity analysis discussion. This acronym indicates both the functional process ("ero", water erosion and deposition; "pwc", physical weathering constants, "cwc", chemical weathering constants; "clay", clay translocation; "bio", bioturbation; "carb", carbon cycle) and the individual parameter itself.

3. Experiments

To avoid idiosyncrasy, exploratory model runs and sensitivity analysis were performed on an hypothetical landscape of 101 by 51 cells of 20 m cellsize (2.06 km^2, Fig. 3). The landscape is symmetrical, with a slope along the axis of symmetry of 0.75% and slopes to both sides of the symmetry axis steepening from flat to 5 percent steep at the edges of the grid.

Soil parent material in this landscape was set to a thickness of 80 m, which for the purposes of this study is infinite (Table 2). Soil parent material was set as an equal mix of the coarse, sand, silt and clay grain size classes, with fine clay and organic matter absent at the start of runs. The specific surface areas for the five texture classes were set at 10 m^2/kg, 100 m^2/kg, 1000 m^2/kg, 50,000 m^2/kg and 100,000 m^2/kg, for the coarse, sand, silt, clay and fine clay classes. Annual rainfall, infiltration and evaporation were set at 0.7, 0.15 and 0.35 m respectively for all cells, to loosely reflect a Mediterranean climate setting. Vegetation was considered absent.

The model was run for 5000 years of combined soil-landscape development with the parameter values and inputs from Tables 1 and 2. The model runtime under these conditions on a standard desktop computer is ca. 0.5 h. Outputs were recorded and are presented below to evaluate model performance. Then parameter values were varied and the model was run repeatedly

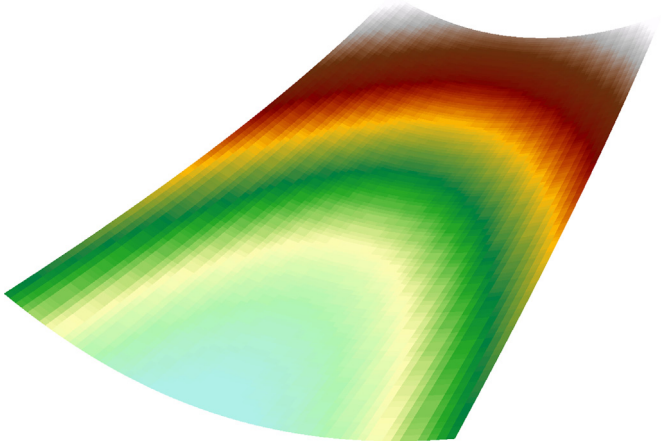

Fig. 3. Input landscape. Suggestion: one-column wide.

Table 2
List of inputs to LORICA.

Input	Unit	Required	Type	Value
Digital Elevation Model	m	yes	Spatial	Fig. 3
Soildepth	m	yes	Scalar/spatial	80 m
Fraction of five grain size classes	Mass fraction	yes	Scalar/spatial	0.25–00.25–00.25–0.25–0
Upper limit of particle size for five texture classes	m	yes		See text
Specific surface area for grain size classes	m^2/kg	only for chemical weathering		See text
Annual rainfall	m	yes	All possible	0.7 m
Annual infiltration	m	yes	All possible	0.15 m
Annual evaporation	m	yes	All possible	0.35 m

for sensitivity analysis. In local sensitivity analysis or one-at-a-time sensitivity analysis, values of one parameter at a time are varied while keeping all others stable. This is often used for landscape evolution models because of the long run times involved (e.g. Claessens et al., 2005; Keijsers et al., 2011; Schoorl et al., 2014). In global sensitivity analysis, all parameters are changed simultaneously (e.g. Saltelli et al., 2000). This delivers more complete information about parameter impact. Given the expected complexity and non-linearity of soilscape dynamics, a global rather than a local sensitivity analysis was performed.

Because of the long model runtime, we used the global screening method proposed by Morris (1991), because it requires relatively few simulations to perform a global sensitivity analysis. Morris (1991) proposed conducting individually randomized experiments that evaluate the elementary effects (relative output differences) of changing one parameter at a time. Each input may assume a discrete number of values, called levels, that are randomly selected within an allocated range of variation for the parameter. For each parameter, two sensitivity measures are proposed: (1) the absolute value of the mean of the elementary effects (μ^*), which estimates the overall effect of the parameter on a given output; and (2) the standard deviation of the effects (σ), which estimates the higher-order characteristics of the parameter (such as curvatures and interactions). Finally, input parameters can be ranked in order of importance by plotting the points on a $\mu^* - \sigma$ plane where influential parameters are farther away from the origin and the less important parameters plot close to the origin.

The number of simulations (n) to perform in the Morris analysis is

$$n = r(k + 1) \tag{24}$$

with r the sampling size for the search trajectory (with satisfactory results for $r > 8$) and k the number of input factors. For this study ($k=28$, $r=10$), this resulted in 290 runs. Values and probability distribution functions (pdf) of input parameters were set based on literature, where possible, and expert knowledge. The range of parameters, reference value and adopted distribution functions are listed in Table 1. Model outputs recorded from all sensitivity runs are presented in Table 3.

Table 3
Model outputs recorded from sensitivity runs.

Model output	Unit	Abbreviation
Total erosion	kg	Total_ero
Total deposition	kg	Total_dep
Net erosion	kg	Net_erosion
Sediment delivery ratio	–	SDR
Physical weathering	kg	Phys_weath
Chemical weathering	kg	Chem_weath
Fine clay formed	kg	Fclay_formed
Fine clay eluviated	kg	Fclay_eluv
Bioturbated mass	kg	Mass_bioturb
Organic matter input	kg	OM_input

4. Results and discussion

Results indicate that several soilscape properties simulated by the model vary in complex ways over time (Fig. 4). Erosion from the catchment and deposition in the catchment is especially complex (Fig. 4A), with large and sudden increases from a minimum value of both variables that increases over time. Although this has not been exhaustively explored in other model outputs, the increases may indicate the effect of breaking through surface armouring and excavation of less protected sediment below it, in parts of the catchment. Similar behaviour was found by Coulthard and Van De Wiel (2007) in simulations with their CAESAR model. In their case, breaking through surface armouring was indeed found to cause this complexity. The results also concur with a recent study by Cohen et al. (2015) who showed that armouring promoted the development of a steady-state soil profile, while under different conditions, for example dominant aeolian soil production processes, spatial variability of steady-state soil profiles was found to be much higher.

The amounts of deposition are low, particularly when compared to erosion. The number of cells with an erosion regime is indeed much larger than the number of cells with a deposition regime–but nonetheless about one in five cells experiences deposition at the end of the experiment (Fig. 4B). The amounts of erosion themselves are also low, indicating relatively successful surface armouring–although the minimum erosion value clearly increases over time. This increase is due to slowly decreasing grain sizes, especially by a shift from the sand grain size class into the smaller grain size classes through chemical weathering, and to increasing connectivity within the landscape, as a drainage pattern develops. Physical weathering (Fig. 4C), which affects the coarse grain size class stronger than chemical weathering does, is less important under the experimental conditions. This could be due partly to the fact that the initial particle size distribution already contains an important fraction of fine material. Physical weathering would probably be more important when considering soil formation from pure bedrock, at least during the initial stage of the weathering process.

As chemical weathering proceeds (Fig. 4D), and increases over time due to the increasing dominance of smaller grain sizes, the formation and eluviation of fine clay also increase (Fig. 4E). Eluviation amounts are higher because eluviation is summed over the various layers that experience the process, and therefore the same amount of clay is counted multiple times, as it passes the various layers. The sudden increases in the amount of eluviation indicate increases in the number of layers, which happen almost simultaneously in many cells in our idealised catchment. They do not reflect or cause increases in the eluviation rate in these layers. Somewhat similarly, the amount of physical weathering shows some sudden drops over time that reflect combining and therefore a change in depth of layers (Eq. (12)). These shortcomings in calculating model outputs are not simply solved by dividing by the number of layers in every cell since layers have no uniform

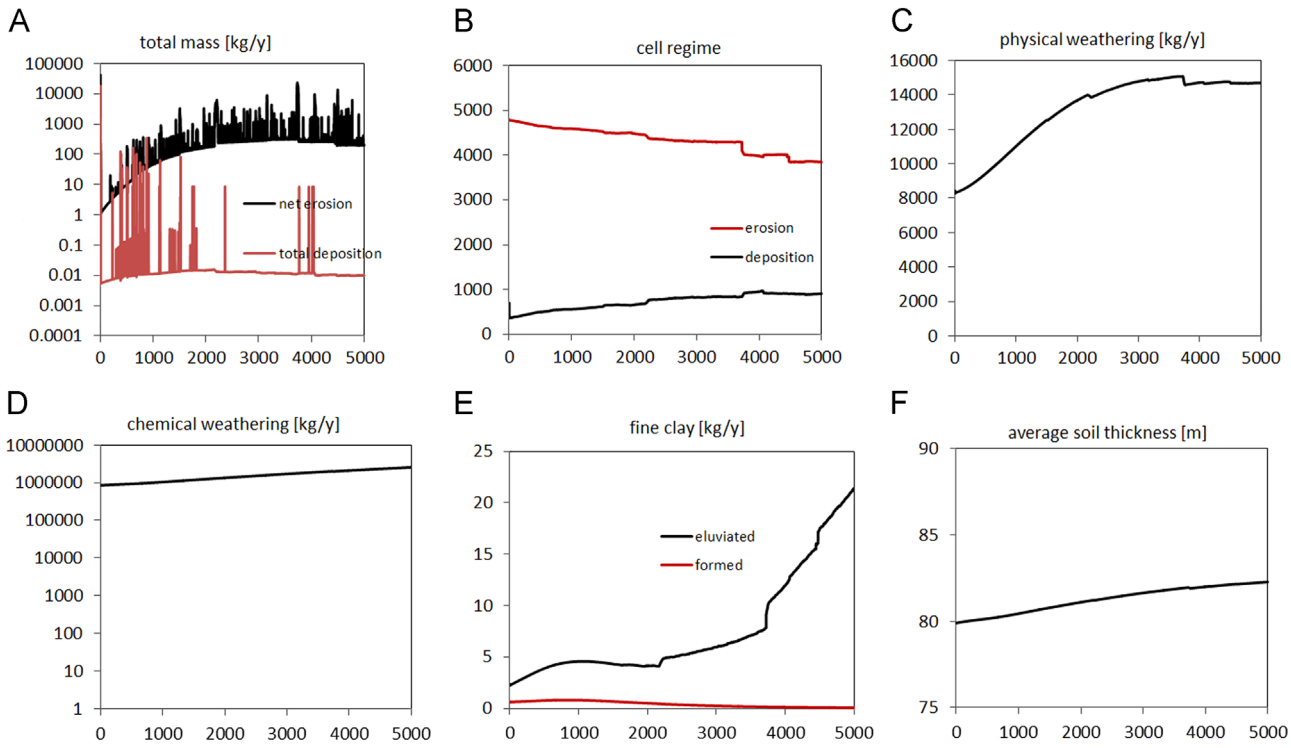

Fig. 4. Timeseries of LORICA outputs.

thickness. A better measure of fine clay eluviation, which is not easily calculated in the current model framework but which would solve this problem, would have units of [kg m/y] to take into account the distance that clay is transported vertically in the profile.

As a result of the overall fining of grain sizes, bulk density of the soil drops over time (Eqs. (1) and (2)), and soils become somewhat thicker as a result. The small amounts of erosion are not enough to balance this effect.

Spatially, a dendritic drainage pattern develops in the experimental catchment, caused by erosion (Fig. 5). Typical values for lowering of the surface in these locations are between 0 and 0.25 m, with values of more than 1 m in a few cells. The raising of the surface in other locations, that are very little affected by erosion (interrill or intergully area), of up to 0.2 m, illustrates the effect of bulk density decrease on the soil surface. Altitude change patterns are not symmetrical due to the effect of small depressions on redistribution patterns. Corresponding clay percentage in the topsoil reflects the fact that uneroded locations lose clay from the topsoil, whereas erosion leads to the exposure of clay-richer layers

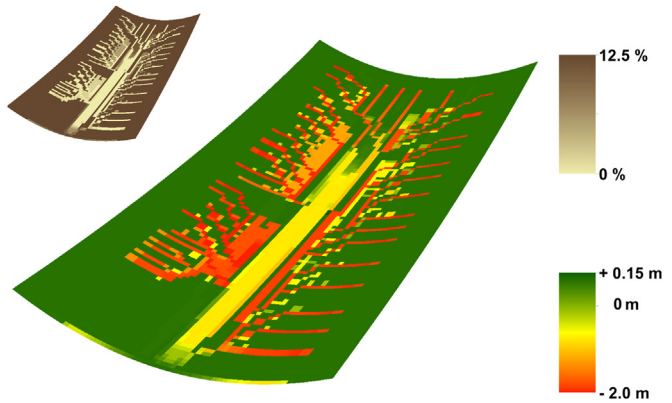

Fig. 5. Map of altitude change in the experimental catchment, and (inset) map of clay percentage in the top soil layer.

in the subsoil, which consequently erode easier. At the same time, armouring leads to a larger fraction of coarse material in the top soil layer (not shown).

Results of the sensitivity analysis are given in terms of the ranking of the input parameters for selected output variables of the LORICA soil-landscape model (Fig. 6). In this set of graphs, the more important the influence of each input parameter, the further away from the origin it plots. For most output variables, only a limited number of input variables could be identified as important.

As expected, the advection erodibility (erok), is identified as an important parameter in the model with respect to soil erosion (net erosion and total_ero). Interestingly, it is not the most important variable. With respect to the four output variables related to erosion and sediment deposition: net erosion, total_dep, total_ero and Sediment Delivery Ratio (SDR), the most important variables include several that are related to profile formation. The parameters controlling the fraction of new clay formation and its depth distribution, respectively, Claycnf and clayc10, are two important variables for net erosion, total_dep and total_ero. This can be explained by the fact that erosion and deposition depend strongly on the particle size distribution of the eroded material, and especially of formation of easily erodible fine new clay. If soil formation processes generate more fines, then more erosion and deposition can take place compared to a coarser soil. This effects was first observed in a modelling experiment by Sharmeen and Willgoose (2006), who also indicated the importance of the granulometry of weathering products in determining whether erosion increases due to weathering (by presence of more fines), or decreases due to weathering (by increasing armouring if weathering products are all of the same grain size).

The balance between erosion and deposition, as expressed by the SDR, depends mostly on the coefficient of the multiple flow factor (erop). This fits with the expression of Eq 4 in flat landscapes such as the experimental catchment: lower values of erop will cause flow to split more evenly between downstream cells, thus lowering the potential for erosion (Eq. (5)). However, two additional input variables, one related to the depth distribution of

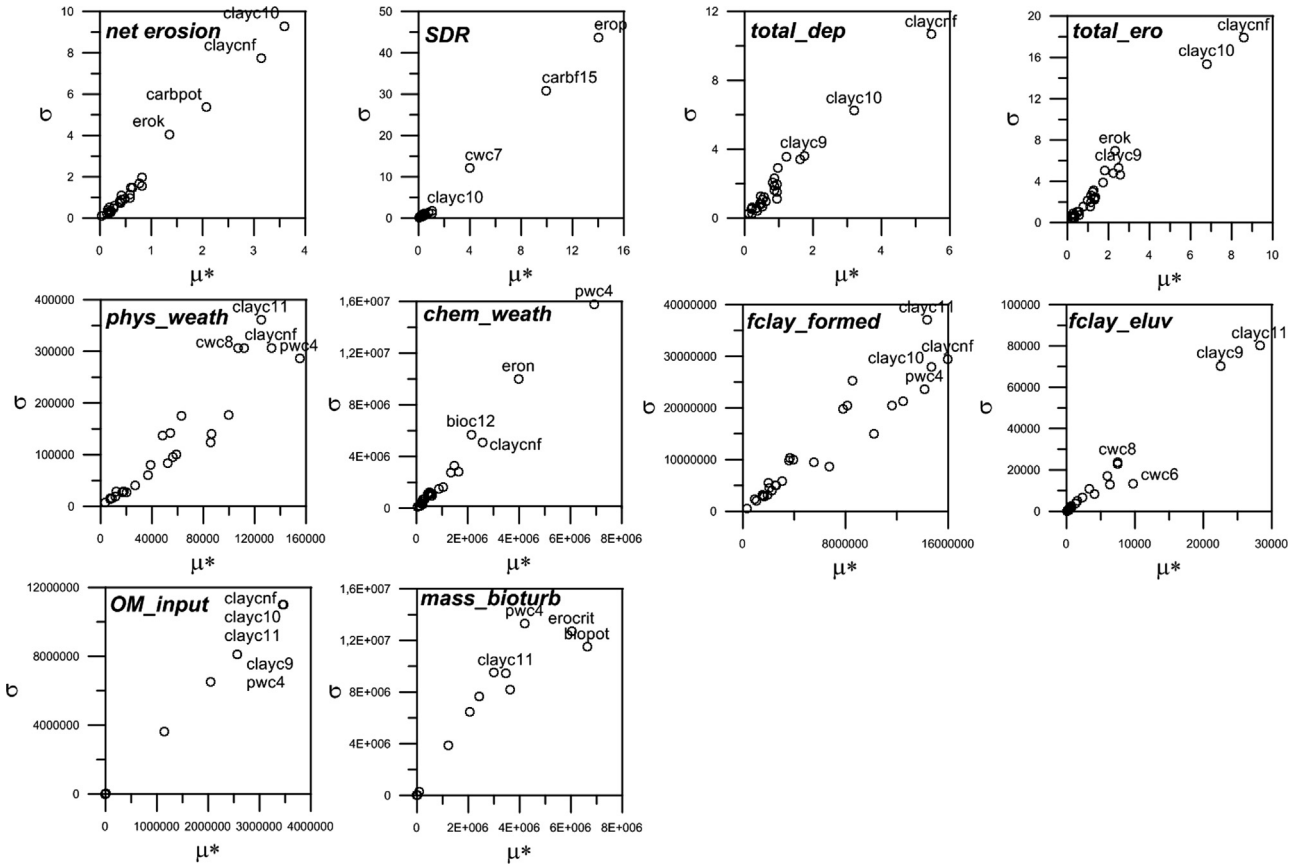

Fig. 6. Global sensitivity analysis results for selected LORICA output variables, obtained using the Morris screening method.

Table 4
Summary of input parameter importance for selected LORICA output variables (only rankings from 1 to 5 are indicated for clarity). The overall relative importance of a parameter was determined by summing the relative importances over all variables. The shaded areas indicate the importance of geomorphic parameters for geomorphic outputs, and of soil parameters for soil outputs. The non-shaded areas provide the opposite: importance from the soil subsystem parameters to the geomorphic subsystem outputs and vice versa.

		Output variable										
		Net ero	SDR	Total_dep	Total_ero	Phys_weath	Chem_weath	Fclay_formed	Fclay_eluv	Mass_bioturb	OM_input	Overall
Parameter	erop	–	1	–	–	–	–	–	–	–	–	–
	erom	–	–	–	–	–	–	–	–	–	–	–
	eron	–	–	–	–	2	–	–	–	5	–	
	erok	4	–	–	3	–	–	–	–	–	–	–
	erocrit	–	–	–	–	–	–	–	–	1	–	–
	eroc1	–	–	4	–	–	–	–	–	–	–	–
	eroc2	–		–	–	–	–	–	–	–	–	–
	erocsel	–	–	–	–	–	–	–	–	–	–	–
	pwc3	–	–	–	–	–	–	–	–	–	1	–
	pwc4	–	–	–	–	4	1	4	4	2	–	4
	pwc5	–	–	–	–	–	–	–	–	–	–	–
	cwc6	–	–	–	–	–	–	–	5	5	5	–
	cwc7	–	3	–	–	–	–	–	–	–	2	–
	cwc8	–	–	–	–	3	–	–	3	–	5	–
	claycnf	2	–	1	1	2	4	2	–	–	–	1
	clayc9	–	–	3	4	5	–	5	2	–	–	5
	clayc10	1	4	2	2	–	–	3	–	–	5	2
	clayctr	–	–	5	5	–	–	–	–	–	–	–
	clayc11	–	–	–	–	1	–	1	1	4	–	3
	biopot	–	–	–	–	–	–	–	–	3	–	–
	bioc12	–	–	–	–	–	3	–	–	–	–	–
	carbpot	3	5	–	–	–	–	–	–	–	5	–
	carbc13	–	–	–	–	–	–	–	–	–	–	–
	carbfhum	5	–	–	–	–	5	–	–	–	2	–
	carbf14	–	–	–	–	–	–	–	–	–	–	–
	carbf15	–	2	–	–	–	–	–	–	–	2	–
	carbf16	–	–	–	–	–	–	–	–	–	–	–
	carbf17	–	–	–	–	–	–	–	–	–	–	–

carbon decomposition (carbc15) and one to the depth distribution of chemical weathering rate (cwc7) are also important.

With respect to physical weathering, all three physical weathering constants were identified as relatively important, with the most important of these being the constant controlling the depth distribution of physical weathering (pwc4). Again, some important interactions with other processes show up within the 5 most important parameters (Table 4). As with erosion, parameters related to fine clay dynamics are among the main parameters. These include the parameters controlling the neoformation of clays (claycnf), a constant controlling the depth distribution of the latter process (clayc9), and the saturation constant or the parameter controlling the proportion of fine clay that is eluviated during each time step (clayc11). One chemical weathering parameter related to the depth distribution of the process (cwc4) was also identified as important.

For chemical weathering, none of the chemical weathering constants come forward as influential. The main parameter here is the physical weathering depth constant (pwc4). Probably, this is due to the fact that chemical weathering is only important for fine particles. As physical weathering controls the conversion from coarse bedrock to fine soil particles, this parameter controls the bottleneck influx of fine particles. Another surprising interaction was found with erosion, as the slope exponent parameter (eron) appears as the second most important parameter. Finally, the parameter controlling the depth distribution of bioturbation rate (bioc12) and the parameter controlling new formation of fine clay (claycnf) appear as third and fourth parameters.

For fine clay formation, a wide range of parameters could be identified to influence the process. First, all relevant parameters related to fine clay dynamics are identified as expected. Interestingly however, the parameter controlling the depth-dependence of physical weathering ranks as the fourth most important (pwc4). Where fine clay eluviation is concerned, only two parameters appear, one controlling the amount of fine clay eluvation itself (the saturation constant, clayc11) and the other controlling the depth-dependence of fine clay formation (clayc9). Other important parameters controlling clay eluviation are related to chemical weathering, with the parameter relating to the specific area coefficient (cwc8) and the weathering rate constant itself (cwc6) and the depth distribution of physical weathering (pwc4).

Unexpectedly, the four most influential parameters related to organic matter input are related to fine clay dynamics (the rate constant of new clay formation, claycnf; the depth distribution of new clay formation, clayc9 and clayc10; and the saturation constant or proportion of fine clay that is eluviated, clayc11) and to the depth distribution of physical weathering (pwc4).

Finally, for bioturbation the three most important parameters are from respectively the potential bioturbation rate (biopot), as expected. However, interactions were found with erosion and physical weathering; the critical erosion threshold parameter (erocrit) and the depth distribution of physical weathering (pwc4) are ranked as the first and second most important variables respectively. The latter can be understood from the biological activity index, which is higher for finer soils. However, the former interaction is hard to explain without further research.

Overall, when summing the importance of the different parameters over all the output variables (Table 4), four out of the five most highly ranked parameters are related to fine clay dynamics (claycnf, clayc9, clayc10 and clayc11). The other parameter is related to physical weathering (pwc4). This again stresses the importance of soil texture, as grain size feeds back into nearly all processes in LORICA. With finer soil texture, more soil can be eroded, a greater surface area is exposed to chemical weathering, and carbon and bioturbation processes are activated. These results also show the importance of the vertical distribution of the intensity of soil formation processes as clayc9, clayc10 and pwc4 all relate to the depth-distribution of respectively clay neoformation and physical weathering. The parameters claycnf and clayc11 control the rate of clay neoformation and of clay eluviation as discussed earlier. More experimental research will therefore have to be done on constraining not only absolute process rates but also their vertical distribution within profiles. For the case of bioturbation for example, promising results seem to be generated by combining Optically Stimulated Luminescencence and Be inventories. By applying this novel technique to soils in Queensland, Australia (Johnson et al., 2014) found a non-linear decrease of mixing rate with increasing soil depth.

The sensitivity analysis shows a way to assess how important interactions between soil formation and landscape evolution processes are. Judging from the ranking of individual parameters, soil and geomorphic parameters are about equally important in determining soil development outputs, whereas soil parameters (particularly those related to fine clay dynamics) are more important than geomorphic parameters in determining landscape dynamics outputs (Table 4). Clearly, this interpretation is sensitive to our hypothetical landscape and soil starting conditions, with equal proportions of all size fractions, and moreover changes significantly over time (Fig. 4). The complexity of the interaction between soil formation and landscape evolution was already shown in a modelling study by Sharmeen and Willgoose (2006). With their model ARMOUR, they observed a fast change in the grading of the surface armouring layer, but very different outcomes depending on the dominant weathering process considered. Surprising interactions appeared between the grading of the weathering products, that of the armouring and the resulting soil erosion rates. This shows that the formation of a small surface armour layer can have a drastic effect on long-term landscape evolution and any change in weathering conditions or in surface runoff generation, for example due to climatic variation, could have a complex response. In a recent study by Cohen et al. (2015), using the new model marm5D, a constant linear hillslope was used during the simulation under the argument that soils typically develop faster than landscapes, and that their development can therefore be simulated on stable landscapes. This implies that changes in soil depth dominate over changes in topography, and there are certainly conditions where this might hold, especially in areas of low erosion rates. However, a clear case where field observations show that this is not the case, is under agricultural land use, where heavily truncated soils are readily observed and landscape evolution clearly dominates. In our case, both soil formation and landscape evolution related parameters appear to have the same order of magnitude importance in driving a co-evolving soil–landscape system. It appears reasonable to expect that (tectonic, climatic, lithologic) circumstances occur in which soils develop faster, at approximately similar speeds, and slower than landscapes. It is of considerable interest to land managers and policy makers to know which of these three possibilities occurs where. In addition, it would be interesting to investigate how vegetation modulates this response. At present, little quantitative research has been done on the interaction soil–landscape-vegetation. Research on the interaction between landscape evolution and vegetation has shown a substantial effect. Modelling vegetation evolution with and without vegetation results in totally different landscapes (Istanbulluoglu and Bras, 2005). Vice versa, erosion and deposition have shown to exert a critical control on vegetation organization (Saco and Moreno-De Las Heras, 2013) As soils are paramount for vegetation establishment and different soil types support different plant functional types, it can be expected (Dietrich and Perron, 2006) that such results will be accentuated when considering soil formation in these interactions. Soil-landscape models such as LORICA, presented here, Marm5D (Cohen et al.,

2015) or MILESD (Vanwalleghem et al., 2013), and additional field observations to parametrize them, can help in this pursuit.

5. Conclusions

We presented LORICA, a new model that simulates the combined evolution of soils and landscapes. It combines a landscape evolution module based on the existing model LAPSUS and a soil formation module based on MILESD. The main novelties of LORICA compared to these models are the significantly higher number of soil layers, the dynamic evolution of the number of layers, depending on the heterogeneity of the soil profile during the simulation, the vegetation and armouring feedbacks on the erosion process and the size-selectivity of sediment transport. Exploratory model runs for an idealized experimental catchment show that the model can combine various soil forming processes and erosion or deposition caused by overland flow, and that complex soil formation and landscape evolution dynamics result from this combination. Sensitivity analysis of the effect of parameters on various model outputs indicated a rich interaction between soil forming factors and the evolution of the surface. Overall, soil parameters appeared to drive geomorphic evolution a bit more than geomorphic parameters did, whereas both groups of parameters appeared to drive soil evolution about equally strongly. A strong influence was found of processes controlling the generation of fine clay particles on the erosion process. As such, landscape evolution could be considered supply-limited, not so much by the weathering of bedrock into soil but by the different soil formation processes that seem to constitute a bottleneck for producing easily erodible fines. Another set of dominant parameters indicate the important depth-dependence of soil formation processes, such as physical weathering and clay neoformation. These results, admittedly obtained from hypothetical boundary conditions, run counter to recent arguments in literature that landscape development is not of relevance to soil development. Further research in different environments, and combining field and model data, will have to show if the results presented here can be generally observed or not.

Acknowledgements

Tom Vanwalleghem acknowledges funding by the Spanish ministry of economy and Competitiveness (through the fellowship Ramón y Cajal RYC-2010-07166 and the research project AGL2012-40128-C03-02). The authors acknowledge the helpful comments of an anonymous reviewer, Gary Willgoose and of Albert Kettner.

References

Amenu, G.G., Kumar, P., Liang, X.-Z., 2005. Interannual variability of deep-layer hydrologic memory and mechanisms of its influence on surface energy fluxes. J. Clim. 18 (23), 5024–5045.
Anderson, R.S., Anderson, S.P., Tucker, G.E., 2013. Rock damage and regolith transport by frost: an example of climate modulation of the geomorphology of the critical zone. Earth Surf. Process. Landf. 38, 299–316.
Anderson, S.P., Hinckley, E.-L., Kelly, P., Langston, A., 2014. Variation in critical zone processes and architecture across slope aspects. Procedia Earth Planet. Sci. 10, 28–33.
Anderson, S.P., von Blanckenburg, F., White, A.F., 2007. Physical and chemical controls on the critical zone. Elements 3 (5), 315–319.
Baisden, W., Amundson, R., Cook, A., Brenner, D., 2002. Turnover and storage of C and N in five density fractions from California annual grassland surface soils. Global Biogeochem. Cycles 16 (4), 64-1–64-16.
Barshad, I., 1959. Factors affecting clay formation. Clays Clay Miner. 6, 110–132.
Braakhekke, M.C., Beer, C., Hoosbeek, M.R., Reichstein, M., Kruijt, B., Schrumpf, M., Kabat, P., 2011. SOMPROF: a vertically explicit soil organic matter model. Ecol. Model. 222 (10), 1712–1730.
Canti, M., 2003. Earthworm activity and archaeological stratigraphy: a review of products and processes. J. Archaeol. Sci. 30 (2), 135–148.
Chittleborough, D., Walker, P., Oades, J., 1984. Textural differentiation in chronosequences from eastern Australia, I. Descriptions, chemical properties and micromorphologies of soils. Geoderma 32 (3), 181–202.
Claessens, L., Heuvelink, G.B.M., Schoorl, J.M., Veldkamp, A., 2005. DEM resolution effects on shallow landslide hazard and soil redistribution modelling. Earth Surf. Process. Landf. 30 (4), 461–477.
Cohen, S., Willgoose, G., Hancock, G., 2010. The mARM3D spatially distributed soil evolution model: three-dimensional model framework and analysis of hillslope and landform responses. J. Geophys. Res. 115 (F04013).
Cohen, S., Willgoose, G., Svoray, T., Hancock, G., Sela, S., 2015. The effects of sediment transport, weathering, and aeolian mechanisms on soil evolution. J. Geophys. Res. F: Earth Surf. 120 (2), 260–274.
Collins, D.B.G., Bras, R.L., Tucker, G.E., 2004. Modeling the effects of vegetation-erosion coupling on landscape evolution. J. Geophys. Res.: Earth Surf. 109 (F3).
Coulthard, T.J., Van de Wiel, M.J., 2006. A cellular model of river meandering. Earth Surf. Process. Landf. 31 (1), 123–132.
Coulthard, T.J., Van De Wiel, M.J., 2007. Quantifying fluvial non linearity and finding self organized criticality? Insights from simulations of river basin evolution. Geomorphology 91 (3–4), 216–235.
Davy, P., Lague, D., 2009. Fluvial erosion/transport equation of landscape evolution models revisited. J. Geophys. Res. B: Solid Earth 114 (3).
Dietrich, W.E., Perron, J.T., 2006. The search for a topographic signature of life. Nature 439 (7075), 411–418.
Ewing, S.A., Sanderman, J., Baisden, W.T., Wang, Y., Amundson, R., 2006. Role of large-scale soil structure in organic carbon turnover: evidence from California grassland soils. J. Geophys. Res.: Biogeosci. 111 (G3) 2005–2012.
Finke, P.A., Hutson, J.L., 2008. Modelling soil genesis in calcareous loess. Geoderma 145 (3–4), 462–479.
Finke, P.A., Vanwalleghem, T., Opolot, E., Poesen, J., Deckers, J., 2013. Estimating the effect of tree uprooting on variation of soil horizon depth by confronting pedogenetic simulations to measurements in a Belgian loess area. J. Geophys. Res. 118, 2013JF002829.
Förster, H., Wunderlich, J., 2009. Holocene sediment budgets for upland catchments: the problem of soilscape model and data availability. Catena 77 (2), 143–149.
Freeman, T.G., 1991. Calculating catchment area with divergent flow based on a regular grid. Comput. Geosci. 17 (3), 413–422.
Goren, L., Willett, S.D., Herman, F., Braun, J., 2014. Coupled numerical–analytical approach to landscape evolution modeling. Earth Surf. Process. Lanf. 39 (4), 522–545.
Hjulström, F., 1935. Studies of the Morphological Activity of Rivers as Illustrated by the River Fyris: Inaugural Dissertation. 10. Almqvist & Wiksells, Stockholm, Sweden.
Holmgren, P., 1994. Multiple flow direction algorithms for runoff modelling in grid based elevation models: an empirical evaluation. Hydrol. Process. 8 (4), 327–334.
Istanbulluoglu, E., Bras, R.L., 2005. Vegetation-modulated landscape evolution: effects of vegetation on landscape processes, drainage density, and topography. J. Geophys. Res. F: Earth Surf. 110 (2).
Johnson, M.O., Mudd, S.M., Pillans, B., Spooner, N.A., Keith Fifield, L., Kirkby, M.J., Gloor, M., 2014. Quantifying the rate and depth dependence of bioturbation based on optically-stimulated luminescence (OSL) dates and meteoric 10Be. Earth Surf. Process. Landf. 39 (9), 1188–1196.
Keijsers, J., Schoorl, J., Chang, K.-T., Chiang, S.-H., Claessens, L., Veldkamp, A., 2011. Calibration and resolution effects on model performance for predicting shallow landslide locations in Taiwan. Geomorphology 133 (3), 168–177.
Legros, J.P., 1982. L'Évolution Granulometrique au Course de la Pedogénèse (Ph.D. thesis). University of Science and Technology, Montpellier.
Maher, K., 2010. The dependence of chemical weathering rates on fluid residence time. Earth Planet. Sci. Lett. 294 (1), 101–110.
Maher, K., Steefel, C.I., White, A.F., Stonestrom, D.A., 2009. The role of reaction affinity and secondary minerals in regulating chemical weathering rates at the Santa Cruz Soil Chronosequence, California. Geochim. Cosmochim. Acta 73 (10), 2804–2831.
McBratney, A.B., Minasny, B., Cattle, S.R., Vervoort, R.W., 2002. From pedotransfer functions to soil inference systems. Geoderma 109 (1–2), 41–73.
Minasny, B., Finke, P., Stockmann, U., Vanwalleghem, T., McBratney, B., in press. How does soil shape the landscape? Earth-Science Reviews, 2015.
Minasny, B., McBratney, A.B., 1999. A rudimentary mechanistic model for soil production and landscape development. Geoderma 90, 3–21.
Minasny, B., McBratney, A.B., Salvador-Blanes, S., 2008. Quantitative models for pedogenesis: a review. Geoderma 144 (1–2), 140–157.
Morris, M.D., 1991. Factorial sampling plans for preliminary computational experiments. Technometrics 33 (2), 161–174.
Pachepsky, Y.A., Rawls, W.J., Lin, H.S., 2006. Hydropedology and pedotransfer functions. Geoderma 131 (3–4), 308–316.
Parker, G., Klingeman, P.C., 1982. On why gravel bed streams are paved. Water Resour. Res. 18 (5), 1409–1423.
Saco, P.M., Moreno-De Las Heras, M., 2013. Ecogeomorphic coevolution of semiarid hillslopes: emergence of banded and striped vegetation patterns through interaction of biotic and abiotic processes. Water Resour. Res. 49 (1), 115–126.
Saltelli, A., Chan, K., Scott, M., 2000. Sensitivity Analysis. John Wiley & Sons, New York.

Salvador-Blanes, S., Minasny, B., McBratney, A.B., 2007. Modelling long-term in situ soil profile evolution: application to the genesis of soil profiles containing stone layers. Eur. J. Soil Sci. 58 (6), 1535–1548.

Schoorl, J.M., Temme, A.J.A.M., Veldkamp, T., 2014. Modelling centennial sediment waves in an eroding landscape – catchment complexity.

Schoorl, J.M., Veldkamp, A., 2001. Linking land use and landscape process modelling: a case study for the Alora region (south Spain). Agric. Ecosyst. Environ. 85 (1–3), 281–292.

Schoorl, J.M., Veldkamp, A., Bouma, J., 2002. Modeling water and soil redistribution in a dynamic landscape context. Soil Sci. Soc. Am. J. 66 (5), 1610–1619.

Sharmeen, S., Willgoose, G.R., 2006. The interaction between armouring and particle weathering for eroding landscapes. Earth Surf. Process. Landf. 31 (10), 1195–1210.

Shields, A., 1936. Anwendung der Aehnlichkeitsmechanik und der Turbulenzforschung auf die Geschiebebewegung [Application of Similarity Mechanics and Turbulence Research on Shear Flow]. Preußische Versuchsanstalt für Wasserbau, Berlin.

Smeck, N.E., Ritchie, A., Wilding, L., Drees, L., 1981. Clay accumulation in sola of poorly drained soils of western Ohio. Soil Sci. Soc. Am. J. 45 (1), 95–102.

Soil Survey Staff, 1999. Soil taxonomy: A Basic System of Soil Classification for Making and Interpreting Soil Surveys. Natural Resources Conservation Service, Washington D.C..

Sommer, M., Gerke, H.H., Deumlich, D., 2008. Modelling soil landscape genesis: a "time split" approach for hummocky agricultural landscapes. Geoderma 145 (3–4), 480–493.

Temme, A.J.A.M., Claessens, L., Veldkamp, A., Schoorl, J.M., 2011. Evaluating choices in multi-process landscape evolution models. Geomorphology 125 (2), 271–281.

Temme, A.J.A.M., Schoorl, J.M., Veldkamp, A., 2006. Algorithm for dealing with depressions in dynamic landscape evolution models. Comput. Geosci. 32 (4), 452–461.

Temme, A.J.A.M., Veldkamp, A., 2009. Multi-process Late Quaternary landscape evolution modelling reveals lags in climate response over small spatial scales. Earth Surf. Process. Landf. 34 (4), 573–589.

Tranter, G., Minasny, B., McBratney, A.B., Murphy, B., McKenzie, N.J., Grundy, M., Brough, D., 2007. Building and testing conceptual and empirical models for predicting soil bulk density. Soil Use Manag. 23 (4), 437–443.

Tucker, G.E., Hancock, G.R., 2010. Modelling landscape evolution. Earth Surf. Process. Landf. 35 (1), 28–50.

Van de Wiel, M.J., Coulthard, T.J., Macklin, M.G., Lewin, J., 2007. Embedding reach-scale fluvial dynamics within the CAESAR cellular automaton landscape evolution model. Geomorphology 90 (3–4), 283–301.

Vanwalleghem, T., Stockmann, U., Minasny, B., McBratney, A.B., 2013. A quantitative model for integrating landscape evolution and soil formation. J. Geophys. Res. F: Earth Surf. 118 (2), 331–347.

Vincent, K.R., Chadwick, O.A., 1994. Synthesizing bulk density for soils with abundant rock fragments. Soil Sci. Soc. Am. J. 58 (2), 455–464.

Wells, T., Willgoose, G., Hancock, G., 2008. Modeling weathering pathways and processes of the fragmentation of salt weathered quartz-chlorite schist. J. Geophys. Res.: Earth Surf. 113 (F1) (2003–2012).

Yoo, K., Amundson, R., Heimsath, A.M., Dietrich, W.E., 2006. Spatial patterns of soil organic carbon on hillslopes: Integrating geomorphic processes and the biological C cycle. Geoderma 130 (1–2), 47–65.

Yoo, K., Ji, J., Aufdenkampe, A., Klaminder, J., 2011. Rates of soil mixing and associated carbon fluxes in a forest versus tilled agricultural field: Implications for modeling the soil carbon cycle. J. Geophysi. Res.: Biogeosci. 116 (G1), S149–S153.